Rotational dynamics of simple asymmetric molecules

D. Fragiadakis and C. M. Roland

Naval Research Laboratory, Chemistry Division, Code 6120, Washington DC 20375-5342, USA

Molecular dynamic simulations were carried out on rigid diatomic molecules, which exhibit both α (structural) and β (secondary) dynamics. The relaxation scenarios range from onset behavior, in which a distinct α process emerges on cooling, to merging behavior, associated with two relaxation peaks that converge at higher temperature. These properties, as well as the manifestation of the β peak as an excess wing, depend not only on thermodynamic conditions, but also on both the symmetry of the molecule and the correlation function (odd or even) used to analyze its dynamics. These observations help to reconcile divergent results obtained from different experiments. For example, the β process is more intense and the α-relaxation peak is narrower in dielectric relaxation spectra than in dynamic light scattering or NMR measurements. In the simulations herein, this follows from the weaker contribution of the secondary relaxation to even-order correlation functions, related to the magnitude of the relevant angular jumps.

I. INTRODUCTION

Studies of the supercooled dynamics of small molecules include not only the usual search for universal characteristics but also discovery of a rich diversity in behavior among different systems. Several classifications of glass-forming materials have been proposed that are based on particular relaxation properties: (i) the extent of departure from Arrhenius behavior of the structural relaxation time (e.g., fragile versus strong temperature dependences [1]); (ii) the secondary relaxation present as a resolved peak or subsumed by the structural relaxation dispersion (e.g., type-A versus type-B glass-formers [2]); (iii) the nature of the appearance of the primary peak above T_g and its intersection with the secondary relaxations at higher temperatures (α-onset versus merging scenarios [3]); (iv) thermodynamic scaling and related properties of unassociated molecules versus that of liquids that form complexes such hydrogen-bonded networks [4,5]; and (v) the magnitude of the stretch exponent β_{KWW} and its correlation with other properties [6].

The categorization of liquids according to their properties, as well as the search for universal behavior, presumes that observations are material characteristics. However, some aspects of relaxation depend on the experimental technique used for the measurement. As an example, for many molecular liquids, the intensity of the secondary β-relaxation is much smaller, and the α-relaxation dispersion broader, when measured by dynamic light scattering or NMR, in comparison to results from dielectric spectroscopy [7–14]. The origin of such differences among materials and between experimental techniques is poorly understood, but an understanding is essential in order to connect the dynamic properties to chemical structure. A first step is to determine the effect of basic parameters, such as molecular shape, polarity, etc., on the experimental manifestations of relaxation; this can be accomplished most easily using simulations of model systems. A suitable system should be as simple as possible, while still exhibiting α and β processes exhibiting the behavior observed experimentally.

We have recently studied a family of rigid, asymmetric diatomic molecules [15–17] interacting via a Lennard-Jones potential. These species exhibit, in addition to the main α relaxation, a secondary β process with properties characteristic of a Johari-Goldstein (JG) relaxation [18]; that is, motion that does not involve intramolecular degrees of freedom. Similar molecules that are symmetric [19,20] or almost symmetric [21–24] undergo 180 degree flips, which have a signature in the correlation function different from that observed experimentally, but a possible connection to the JG-process has been noted. A Johari-Goldstein process has also been observed in simulations of bead-spring polymers [25,26].

In this paper we discuss features of the α and β relaxations measured by different orientational correlators, which in experiments are detected by different techniques (first-order correlation function by dielectric spectroscopy, second-order by dynamic light scattering and NMR). We also examine how characteristics such as the temporal separation and spectral breadths of the relaxations depend on the molecular asymmetry. Our results help to rationalize the apparently contradictory findings for such features when measured by different experimental techniques. Physical insights are drawn from analysis of the orientational dynamics in the corresponding van Hove functions.

II. METHODS

Simulations were carried out using the HOOMD simulation package [27,28]. The systems studied are binary mixtures (4000:1000) of rigid, asymmetric, diatomic molecules. Atoms belonging to different molecules interact through the Lennard-Jones potential, using parameters for the Kob-Andersen liquid [29]. Details of the procedure can be found elsewhere [15–17]. In this work we studied a family of molecules with constant bond length ($l = 0.45$) and varying size ratio r of the two particles, from $r = 0.5$ (asymmetric) to 0.875 (nearly symmetric). These parameters and sketches of the corresponding molecular shapes are in Table I.

TABLE I. Four rigid molecules of present study; σ_A and σ_B are the Lennard-Jones size parameters for the large and small particles, respectively.

Shape	Bond length l	Size ratio $r = \sigma_B/\sigma_A$
	0.45	0.5
	0.45	0.625
	0.45	0.75
	0.45	0.875

We study reorientational motions using the first- and second-order rotational correlation functions

$$C_1(t) = \langle \cos \theta(t) \rangle, \qquad (1)$$

$$C_2(t) = \tfrac{1}{2}\langle 3\cos^2\theta(t) - 1 \rangle, \qquad (2)$$

where θ is the angular change of a unit vector along the molecular axis [30]. The same dynamical information is contained in the corresponding susceptibilities, $\chi_1(\omega)$ and $\chi_2(\omega)$, calculated from

$$\chi(\omega) = \chi'(\omega) + i\chi''(\omega) = 1 + i\omega \int_0^\infty dt\, e^{i\omega t} C(t). \qquad (3)$$

In this work we examine the dynamics of the majority species in the mixture (i.e., the larger molecule); the behavior of the minority species was qualitatively the same. Since the simulated species are not intended to represent any particular real molecules, the data are presented in normalized units (Lennard-Jones units) of length σ_{AA}, temperature ε_{AA}/k_B, and time $(m\sigma_{AA}^2/\epsilon_{AA})^{1/2}$.

III. ROTATIONAL RELAXATION

Previously we investigated the dynamics of a series of rigid asymmetric diatomic molecules with $r = 0.5$ and established that they show three distinct motions [16]: the slowest is an α relaxation, and the fastest corresponds to vibrations; at intermediate times there is a secondary process that exhibits the characteristics of the Johari-Goldstein process seen in real liquids [18].

In Fig. 1 we compare the first- and second-order rotational susceptibilities for each of our four liquids. Both susceptibilities show features corresponding to these same three dynamic processes, which from low to high frequencies are the α relaxation, the β relaxation, and vibrational motion. However, the shapes of the two correlation functions are quite different. For all four molecules, χ_1 exhibits the α-onset scenario: At high temperatures there is a single peak at the frequency of the β process. On cooling to an onset temperature T_{on}, the α relaxation emerges as a shoulder on the low-frequency side of the more intense β peak. Thus, with decreasing temperature the relaxation strength of the α process increases at the expense of the β intensity. As r increases, making the molecule longer and more symmetric, the only significant effect on the χ_1 spectrum is that τ_α and τ_β are more nearly equal, and the "α onset" occurs at lower frequencies.

For χ_2, however, the relative intensity of the β process decreases substantially as the molecule becomes more symmetric, leading to a qualitative change from the α-onset
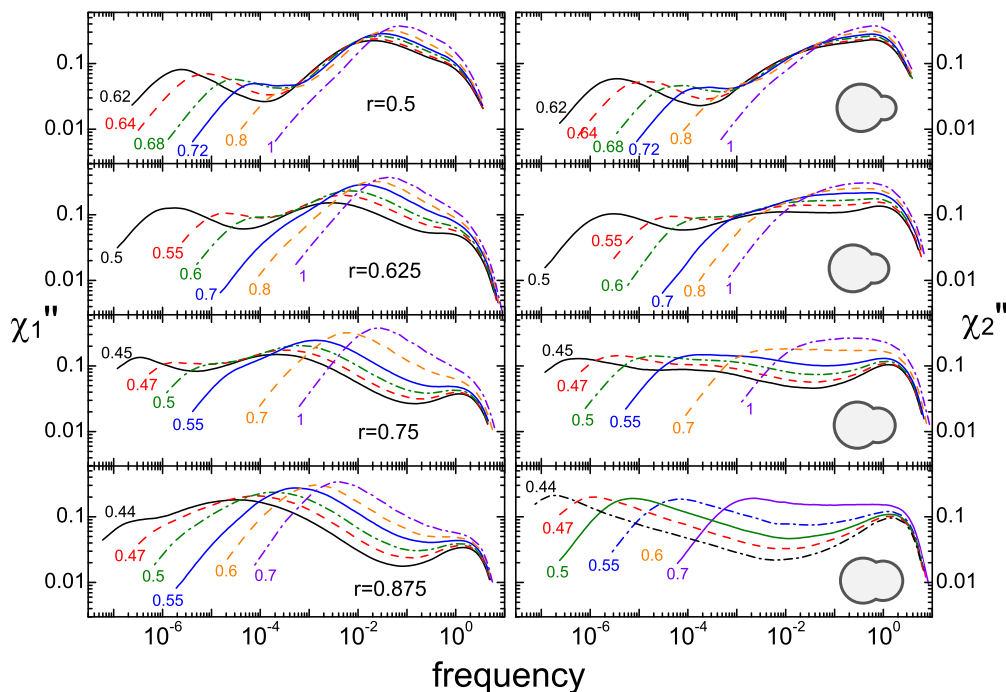

FIG. 1. (Color online) Left: first-order rotational susceptibility as a function of frequency for each liquid at various temperatures. All spectra show α and β relaxations and (at a frequency near unity) vibrations. Right: Corresponding second-order susceptibilities, with the three dynamic modes again evident in the spectra.
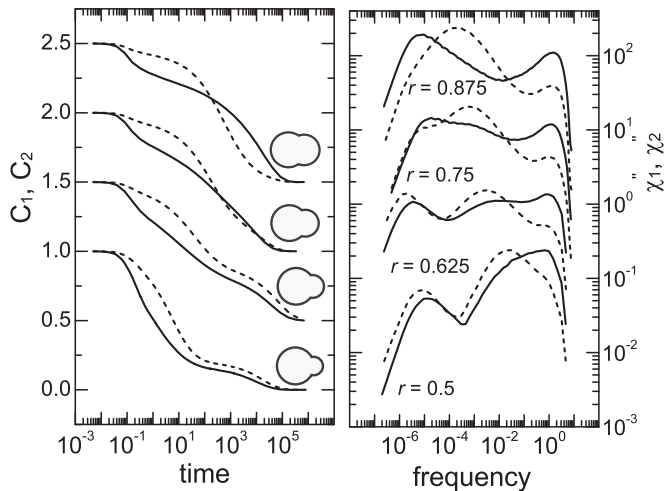
FIG. 2. Left: First-order (dashed lines) and second-order (solid lines) rotational correlation functions for each liquid, at temperatures chosen to give similar α-relaxation times, $\tau_\alpha^{(1)} \sim 10^4$ for $C_1(t)$. Right: Corresponding rotational susceptibilities as a function of frequency. In both panels the curves have been shifted vertically for clarity.
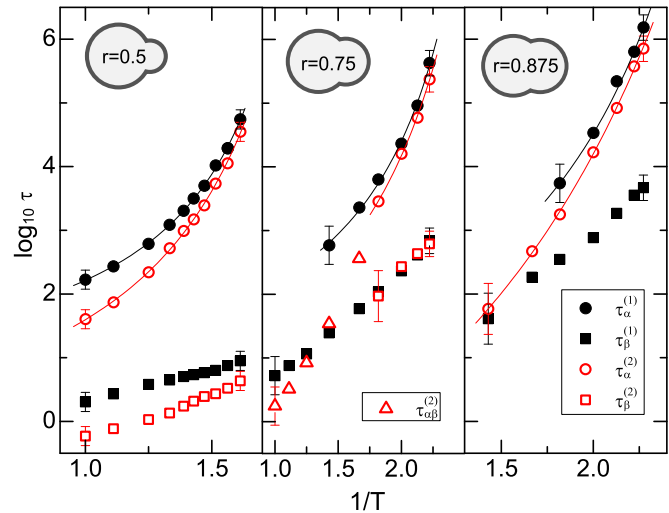

FIG. 3. (Color online) Rotational relaxation times from first-order (filled symbols) and second-order (open symbols) correlation functions. For a given τ_α, separation of the primary (circles) and secondary (squares) decreases with increasing molecular symmetry. The triangles in the middle panel denote the merged $\alpha\beta$ relaxation. Lines are fits of Eq. (5) to the α relaxation times.

scenario (seen in Fig. 1 for $r = 0.5$ and 0.625), to merging of the peaks ($r = 0.75$). For $r = 0.875$, the "excess wing" scenario is observed, presaging the absence of a secondary process for the symmetric case [19]. The vibrational contribution is stronger in χ_2 than in χ_1, since the former emphasizes smaller angle motions. These various characteristics are brought out in Fig. 2, comparing the time correlation functions and the susceptibilities for the four molecules at temperatures for which their τ_α are equal.

For spectra for which the α and β processes are both present, the susceptibilities and correlation functions were analyzed using the Williams ansatz [31]

$$C(t) = \Delta_\alpha C_\alpha(t) + \Delta_\beta C_\alpha(t) C_\beta(t), \qquad (4)$$

in which Δ represents the relaxation strength. This approach assumes the two relaxations decay simultaneously and interdependently. For the relaxation functions we used a stretched exponential (Kohlrausch) equation [32] to fit the α-relaxation and a Cole-Cole function [33] (or its time domain equivalent) for the β. The common alternative to Eq. (4) is to assume the two relaxation functions are additive in the time or frequency domains. In that case the β relaxation herein had to be described using an asymmetric function to provide a satisfactory fit, which requires an additional adjustable parameter. Nevertheless, the additivity assumption gave slightly poorer fits and larger fitting parameter uncertainties than Eq. (4). Since the dynamic heterogeneity of the α and β processes are unrelated [17], both assumptions are plausible. For the present simulated structures, the two approaches yield comparable fit parameters, except when the α- and β-relaxation times are very close (less than an order of magnitude difference), in which case an analysis assuming distinct contributions is questionable, given the breadth of the dispersions. From the fits we obtain the time constants τ_α and τ_β, relaxation strengths Δ_α and Δ_β, the stretch exponent β_{KWW} for the α relaxation, and the shape parameter a_{CC} for the β process.

Relaxation times from the first- and second-order correlation functions are plotted in Fig. 3, where it can be seen that the difference between τ_α and τ_β is reduced and the α-onset timescale becomes longer with greater molecular symmetry (larger r). The origin of this effect is uncertain. Generally, the two processes are closer for weaker intermolecular cooperativity; i.e., a smaller number of molecules moving in a correlated fashion; this affects the α relaxation more strongly than it does the weakly cooperative β process. A decrease in the number of dynamically correlated molecules with increasing molecular length was indeed found for similar molecules in Ref. [17]. For the second-order rotational relaxation times (open symbols), there is a change from "onset" ($r = 0.5$) to "merging" ($r = 0.75$) behavior, and for $r = 0.875$ an "excess wing" becomes apparent. (In this last case, reliable values of $\tau_\beta^{(2)}$ cannot be determined and thus are omitted from Fig. 3).

Comparing the relaxation times for the two correlation functions, $\tau_\alpha^{(2)}$ is always less than $\tau_\alpha^{(1)}$, but this difference decreases at lower temperature. For the secondary relaxations, $\tau_\beta^{(2)}$ is three to four times shorter than $\tau_\beta^{(1)}$ for $r = 0.5$, but the two time constants become more nearly equal with increasing molecular symmetry.

The α relaxation times can be described by the Vogel-Fulcher-Tammann (VFT) equation [32],

$$\tau_a(T) = \tau_0 \exp\left(\frac{B}{T - T_0}\right), \qquad (5)$$

where τ_0, B, and T_0 are temperature-independent fit parameters. In the first-order correlation function of the molecule with $r = 0.75$, the α and β relaxation merge at $T > 0.55$; therefore, a single VFT function cannot describe the data over the entire temperature range. In that case we only fit for $T \leqslant 0.55$, where the α and β processes are separated. At higher temperatures the merged $\alpha\beta$ relaxation has a different temperature dependence.

TABLE II. Fit parameters of Eq. (5) for the temperature dependence of the α-relaxation times from first- and second-order rotational correlation functions.

r	$\log \tau_0^{(1)}$	$B^{(1)}$	$T_0^{(1)}$	$\log \tau_0^{(2)}$	$B^{(2)}$	$T_0^{(2)}$
0.5	1.26	1145	0.48	0.27	1677	0.45
0.625	1.88	732	0.40	0.48	1427	0.35
0.75	1.95	820	0.35	0.64	1618	0.30
0.875	0.63	1792	0.30	-1.39	3348	0.24

Interestingly, the curves for $\tau_{\alpha\beta}^{(2)}$ and $\tau_{\beta}^{(1)}$ intersect, so that at the highest temperatures $\tau_{\alpha\beta}^{(2)} < \tau_{\beta}^{(1)}$. This can be understood by considering the temperature variation of the intensities of the α and β processes. Herein, as is the case for the species studied in Ref. [16] and as is commonly found in dielectric spectroscopy experiments [32], the intensity of the α relaxation decreases with increasing temperature, but that of the β relaxation increases. Although the merged $\alpha\beta$ process cannot be resolved into separated α and β processes, both α- and β-type motions will exist within it, their respective contributions increasing and decreasing with increasing temperature. This means that at the highest temperatures, the merged peak is essentially the β process, whereby $\tau_{\alpha\beta}^{(2)}$ can be shorter than $\tau_{\beta}^{(1)}$, as is the case for the β processes for $r = 0.5$ and $r = 0.625$.

A note on the timescales involved: the susceptibility peak corresponding to vibrational motions (see Fig. 1) occurs at a temperature-independent frequency on the order of unity in Lennard-Jones units. For real materials the corresponding peak frequency is typically around 10^{12} Hz [34,35], so that herein a Lennard-Jones time unit equal to one corresponds to about 1 ps. Thus, the longest relaxation times herein are on the order of a few microseconds on an experimental time scale. In principle it is be possible to use Eq. (5) to extrapolate to the long times associated with an experimental glass transition temperature T_g; i.e., $\tau_\alpha(T_g) = 100$ s, which is about 10^{14} Lennard-Jones units. Besides requiring an extrapolation of at least eight orders of magnitude, this ignores the possibility of a crossover to a different temperature dependence of τ_α at temperatures lower than the ones simulated. Such dynamic crossovers are widely observed in experiments on real liquids [36], and there is indirect evidence of such in simulated simple liquids [37].

The fit parameters for Eq. (5) are shown in Table II. For all molecules studied, the temperature dependence of $\tau_\alpha^{(2)}$ is characterized by a higher effective activation energy (larger B) and slightly lower Vogel temperature, T_0, compared to those of $\tau_\alpha^{(1)}$. The same trend was observed in a comparison of dielectric spectroscopy and light-scattering data, which yield $\tau_\alpha^{(1)}$ and $\tau_\alpha^{(2)}$, respectively [7]. T_0 decreases systematically with increasing molecular symmetry. For this series of molecules, increasing symmetry also corresponds to increased molecular length, so the behavior of T_0 may be ascribed to packing considerations, as discussed in Ref. [16]. The parameters τ_0 and B show a maximum and minimum, respectively, with increasing r.

The Kohlrausch stretch exponent, which is an (inverse) measure of the breadth of the relaxation dispersion, is plotted in Fig. 4 for the two correlation functions. The behavior of $C_1(t)$ is similar to that observed in our previous simulations of asymmetric-dumbbell-shaped molecules [16]: $\beta_{\text{KWW}}^{(1)}$ increases
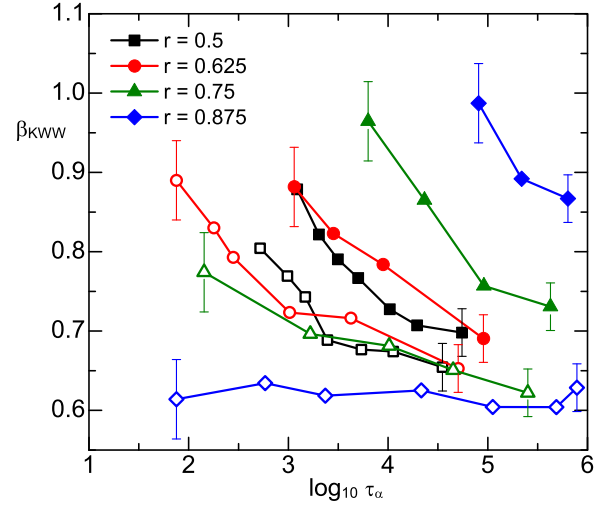

FIG. 4. (Color online) Stretch exponent as a function of α-relaxation time for first-order (filled symbols) and second-order (open symbols) rotational correlation functions.

with increasing temperature (smaller τ_α), approaching unity (exponential decay) at the "α onset." For the second-order correlation function, rotational relaxation is more stretched (smaller exponent), consistent with experimental results for tricresyl phosphate and glycerol, in which comparisons were made of dielectric (χ_1) and light-scattering (χ_2) spectra [12], similar results for several polymers [7–10], and recent atomistic simulations of o-terphenyl [38]. The temperature dependence of $\beta_{\text{KWW}}^{(2)}$ becomes weaker with increasing r, and for $r = 0.875$ the peak breadth is temperature-invariant; that is, the nearly symmetrical case conforms to time-temperature superpositioning. Most experimental studies report increasing β_{KWW} with increasing temperature [39,40], although in some cases a temperature-independent β_{KWW} has been observed [12]. The origin of the different behaviors is unknown. The situation is complicated when the α- and β-relaxation times are within a few decades of each other, since the magnitude and temperature dependence of β_{KWW} will depend on the method used to deconvolute the peaks. As stated, herein Eq. (4) was applied for temperatures for which both peaks were present in the spectra.

The symmetric version of these molecules ($r = 1.0$, with various bond lengths) has been studied by Moreno *et al.* [41]. They found the α process was only evident in the second-order susceptibility, for which, however, the β process was absent. The first-order susceptibility had only a single peak, which resembles the β relaxation. This is due to the fact that the secondary process in symmetric molecules consists of 180-degree flips. Such flips contribute to a decay of the odd-order correlation function, but make no contribution to $C_2(t)$. This suggests that the different behavior of the odd and even correlation functions is governed by the magnitude of the angular jumps comprising the β dynamics. These magnitudes can be quantified using the self-part of the angular van Hove function [22]:

$$G_s^\theta(\theta, t) = \frac{2}{N \sin \theta} \sum_{i=1}^{N} \delta[\theta - \theta_i(t)]. \quad (6)$$
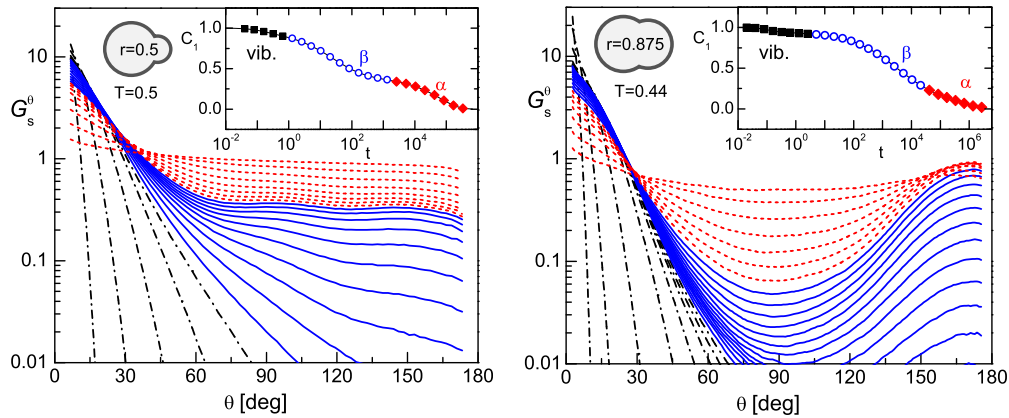
FIG. 5. (Color online) G_s^θ at various times for $r = 0.5$ at $T = 0.5$ (left) and $r = 0.875$ at $T = 0.44$ (right). The inset shows the first-order rotational correlation function for the same temperatures and times. Each G_s^θ curve corresponds to one of the points in the inset. As a visual aid we distinguish three different regimes, dominated by the three relaxations: (i) vibrational motions at short times (filled squares, dash-dotted lines); (ii) β relaxation at intermediate times (open circles, solid lines); and (iii) α relaxation at long times (filled diamonds, dotted lines).

The probability that the molecular axis lies at an angle between θ and $\theta + d\theta$ at time t for an initial orientation $\theta = 0$ at $t = 0$ is $\frac{1}{2} G_s^\theta(\theta, t) \sin \theta \, d\theta$. At long times G_s^θ goes to unity, since all orientations are equally probable.

In Fig. 5 G_s^θ is plotted for two species representing the extremes in molecular symmetry herein. We can distinguish three regimes, dominated respectively by vibrations, the secondary relaxation, or the α process. At short times, corresponding to vibrational motion, the molecules explore a relatively narrow range of angles in a continuous way. At intermediate times (secondary relaxation) the incidence of large angular jumps increases, with the development of one or more peaks in G_s^θ, particularly for the more symmetric molecule. These peaks are most distinct at the timescale of the β process. Finally, at longer times (isotropic α dynamics) the peaks dissipate and G_s^θ flattens, approaching a value of unity.

In Fig. 6 are G_s^θ for each molecule type near the end of their β-relaxation regime. At that time the peaks corresponding to large-angle jumps are most distinct, since they have nearly

fully developed but have not yet begun to decay (this decay coincides with the onset of the α relaxation). For the nearly symmetric structure ($r = 0.875$), $\sim$ 180-degree flips are strongly favored, with consequently a single prominent peak near 180 degrees. The molecule with $r = 0.75$ behaves in much the same way, but with a broader, less-intense peak at large angles. For more asymmetric molecules ($r = 0.625$ and 0.5), 180-degree flips no longer dominate the β relaxation; rather, the jumps occur over a broad angular range. Multiple, weak peaks appear in G_s^θ, indicating that the preferred jumps are mostly in the range of 90–150 degrees. At the timescale of Fig. 6, translational motion of the molecular center of mass is not yet significant, since it occurs at much longer times via the α process. Each molecule's neighbors are undergoing vibrations and orientational jumps, but their center of mass is relatively fixed; the material at this timescale is essentially a glass. The peaks in G_s^θ, therefore, can be interpreted as the angles between energetically favorable orientations of the molecules within the quasistatic potential created by the neighbors.

This information about the angular displacements associated with large reorientations of different molecules can aid interpretation of the differences between the first- and second-order rotational correlation functions. Jumps of 180 degrees enable C_1 to relax but leave C_2 unaffected. Therefore, in the case of such large jumps, the β relaxation in C_1 has a larger amplitude than in C_2, and the α relaxation is correspondingly weaker. Conversely, smaller jumps cause a larger change in C_2 than in C_1, and therefore a larger amplitude for the β relaxation in C_2.
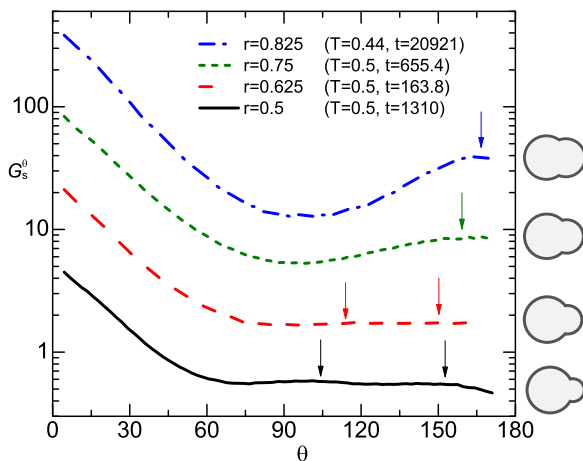

FIG. 6. (Color online) Van Hove function for each molecule, at a time near the end of the β-relaxation regime, where the large-angle jumps are most prominent. Approximate positions of the peaks (indicated by arrows) are sensibly independent of t. Curves have been shifted vertically for clarity (decreasing r from top to bottom).

IV. DISCUSSION AND SUMMARY

Measuring the dynamics of liquids and polymers using different experimental techniques (dielectric spectroscopy, light scattering, nuclear magnetic resonance, and mechanical spectroscopy) often yields differences in the response. Such differences are important because in characterizing and classifying liquids, it is critical to focus on true material properties, rather than aspects of the behavior that depend on the experimental probe. At the same time, understanding the

origin of the differences can offer insights into the molecular mechanisms underlying the measured dynamics.

Many of the differences arise in part due to the different correlation functions relevant to different techniques. The present work focused on the orientational correlation functions: $C_1(t)$ in dielectric spectroscopy measurements and $C_2(t)$ in depolarized light scattering and nuclear magnetic resonance experiments. The literature [7,8–14] reveals that in comparison to dielectric spectroscopy, light scattering yields longer or equal α-relaxation times (although the opposite is sometimes found in certain polymers [7]) and a smaller, or equal, stretch exponent β_{KWW}. In addition, the VFT temperature dependence of τ_α is characterized by a larger parameter B [Eq. (5)] in light scattering than for dielectric spectroscopy.

The secondary relaxation can also exhibit different behavior for different experimental techniques. In 2-picoline, dimethylphosphate, and salol, the intensity of the secondary relaxation, relative to that of the α process, is much less in dynamic light-scattering spectra than in dielectric spectra [12]. For the glass-forming liquid diglycidyl ether of bisphenol A (DGEBA), a β peak is only seen in dielectric measurements [14]. On the other hand, in glycerol and m-tricresyl phosphate the excess wing is weaker in the dielectric spectra [12,14].

In this work, we chose to simulate the simplest possible structure that results in α and β relaxations with the characteristics observed experimentally. Compared to real liquids, these diatomic molecules have fixed bond lengths and lack any dipole moment. The effect of interactions on the correlation functions C_1 and C_2 is also neglected, as these are calculated based on the average of the corresponding molecular correlation functions [30]. Therefore, care should be taken in applying the results of these simulations to experimental data; a complete accounting for the disparities among dynamic measurements on real materials is certainly beyond the scope of the present paper. Nevertheless, our results illustrate how even for very simple structures, lacking internal degrees of freedom and polarity, molecular motions can give rise to spectral features that differ, *inter alia*, with the order of the correlation function used for the analysis, in ways similar to experimental results. Specifically we find:

(1) The variations in structural relaxation properties such as τ_α and b_{KWW} for different correlation functions are observed in our simulations. The VFT parameters can also be affected,

although the approximate invariance of the product $\beta_{KWW}B$ for different experimental probes, proposed in Ref. [7], does not hold for the data in Table II.

(2) The diversity in the properties of the β relaxation found experimentally is observed in the systems simulated herein. For large r (more symmetric molecules) the β relaxation is much weaker in C_2 than in C_1, while for small r it is equally prominent in the two functions. The effect of experimental probe on the β process seems to be nonuniversal; rather, it depends on the molecular shape.

(3) All species investigated herein show an "α-onset" scenario in the first-order correlation function: with cooling the α peak begins to emerge on the low-frequency side of the dispersion. In contrast, in the second-order function this onset behavior is only found for less symmetric (shorter) molecules. For the more symmetric cases the α peak merges with the β process as temperature increases. For the largest r the intensity of the β process becomes small, manifested in the second-order susceptibility only as an excess wing. These differences in the spectra are due primarily to the weak nature of the β dynamics in C_2 for large r due to the prevalence in the β dynamics of 180-degree flips; these orientation reversals have minimal effect on even correlation functions. It is noteworthy that some species show an excess wing or the opposite behavior ("onset scenario") depending on the correlation function being examined. This implies that classifying liquids according to a type A or type B scenario (i.e., the presence and absence of an excess wing) [2] may not be useful or generally applicable.

(4) Consistent with experimental results, the α relaxation is faster and broader (smaller stretch exponent) in C_2 than in C_1. For the first-order function the stretch exponent increases and its temperature dependence becomes stronger with increasing molecular symmetry. The opposite trend is observed for the second-order correlation function, resulting in a temperature-independent peak shape for the most symmetric molecule.

[1] C. A. Angell, J. Phys. Chem. Solids **49**, 863 (1988).

[2] A. Kudlik, S. Benkhof, T. Blochowicz, C. Tschirwitz, and E. Rössler, J. Mol. Struct. **479**, 201 (1999).

[3] E. Donth, *The Glass Transition: Relaxation Dynamics in Liquids and Disordered Materials* (Springer, New York, 2001).

[4] N. P. Bailey, T. Christensen, B. Jakobsen, K. Niss, N. B. Olsen, U. R. Pedersen, T. B. Schroder, and J. C. Dyre, J. Cond. Phys. Cond Mat. **20**, 244113 (2008).

[5] C. M. Roland, *Viscoelastic Behavior of Rubbery Materials* (Oxford University Press, Oxford, 2011).

[6] S. Capaccioli, M. Paluch, D. Prevosto, L. M. Wang, and K. L. Ngai, J. Phys. Chem. Lett. **3**, 735-743 (2012).

[7] K. L. Ngai, S. Mashimo, and G. Fytas, Macromolecules **21**, 3030 (1988).

[8] C. H. Wang, G. Fytas, D. Lilge, and Th. Dorfmüller, Macromolecules **14**, 1363 (1981).

[9] G. Fytas, A. Patkowski, G. Meier, and Th. Dorfmüller, J. Chem. Phys. **80**, 2214 (1984).

[10] G. Fytas, C. H. Wang, G. Meier, and E. W. Fischer, Macromolecules **18**, 1492 (1985).

[11] A. Brodin, R. Bergman, J. Mattson, and E. A. Rössler, Eur. Phys. J. B **36**, 349 (2003).

[12] N. Petzold, B. Schmidtke, R. Kahlau, D. Bock, R. Meier, B. Micko, D. Kruk, and E. A. Rössler, J. Chem. Phys. **138**, 12A510 (2013).

[13] L. Comez, D. Fioretto, L. Palmieri, L. Verdini, P. A. Rolla, J. Gapinski, T. Pakula, A. Patkowski, W. Steffen, and E. W. Fischer, Phys. Rev. E **60**, 3086 (1999).

[14] C. Gainaru, O. Lips, A. Troshagina, R. Kahlau, A. Brodin, F. Fujara, and E. A. Rössler, J. Chem. Phys. **128**, 174505 (2008).

[15] D. Fragiadakis and C. M. Roland, Phys. Rev. E **86**, 020501(R) (2012).

[16] D. Fragiadakis and C. M. Roland, Phys. Rev. E **88**, 042307 (2013).

[17] D. Fragiadakis and C. M. Roland, Phys. Rev. E **89**, 052304 (2014).

[18] K. L. Ngai and M. Paluch, J. Chem. Phys. **120**, 857 (2004).

[19] A. J. Moreno, S.-H. Chong, W. Kob, and F. Sciortino, J. Chem. Phys. **123**, 204505 (2005).

[20] S.-H. Chong, A. J. Moreno, F. Sciortino, and W. Kob, Phys. Rev. Lett. **94**, 215701 (2005).

[21] S. Kämmerer, W. Kob, and R. Schilling, Phys. Rev. E **56**, 5450 (1997).

[22] C. De Michele and D. Leporini, Phys. Rev. E **63**, 036702 (2001).

[23] M. Higuchi and T. Odagaki, J. Phys. Soc. Jpn. **71**, 735 (2002).

[24] M. Higuchi, J. Matsui, and T. Odagaki, J. Phys. Soc. Jpn. **72**, 178 (2003).

[25] D. Bedrov and G. D. Smith, Phys. Rev. E **71**, 050801(R) (2005).

[26] D. Bedrov and G. D. Smith, J. Non-Cryst. Solids **357**, 258 (2011).

[27] HOOMD web page: http://codeblue.umich.edu/hoomd-blue.

[28] J. A. Anderson, C. D. Lorenz, and A. Travesset, J. Comput. Phys. **227**, 5342 (2008).

[29] W. Kob and H. C. Andersen, Phys. Rev. Lett. **73**, 1376 (1994).

[30] C_1 and C_2 are calculated herein by averaging the rotational correlation functions of the individual molecules. This neglects orientational correlations between molecules, which may contribute to experimental data from, for example, dielectric spectroscopy.

[31] G. Williams, Adv. Polym. Sci. **33**, 59 (1979).

[32] F. Kremer and A. Schonhals, *Broadband Dielectric Spectroscopy* (Springer, New York, 2003).

[33] K. Cole and R. Cole, J. Chem. Phys. **9**, 341 (1941).

[34] U. Schneider, P. Lunkenheimer, R. Brand, and A. Loidl, J. Non-Cryst. Solids **235-237**, 173 (1998).

[35] U. Schneider, P. Lunkenheimer, R. Brand, and A. Loidl, Phys. Rev. E **59**, 6924 (1999).

[36] F. Stickel, E. W. Fischer, and R. Richert, J. Chem. Phys. **102**, 6251 (1995).

[37] El. Flenner and G. Szamel, J. Chem. Phys. **138**, 12A523 (2013).

[38] M. P. Eastwood, T. Chitra, J. M. Jumper, K. Palmo, A. C. Pan, and D. E. Shaw, J. Phys. Chem. B. **117**, 12898 (2013).

[39] R. Casalini, K. L. Ngai, and C. M. Roland, Phys. Rev. B **68**, 014201 (2003).

[40] C. León and K. L. Ngai, J. Phys. Chem. B **103**, 4045 (1999).